

Supernova Search with the AMANDA / IceCube Detectors

Thomas Kowarik*, Timo Griesel*, Alexander Pięgsa* for the IceCube Collaboration[†]

* *Institute of Physics, University of Mainz, Staudinger Weg 7, D-55099 Mainz, Germany*

[†] <http://www.icecube.wisc.edu/collaboration/authorlists/2009/4.html>

Abstract. Since 1997 the neutrino telescope AMANDA at the geographic South Pole has been monitoring our Galaxy for neutrino bursts from supernovae. Triggers were introduced in 2004 to submit burst candidates to the Supernova Early Warning System SNEWS. From 2007 the burst search was extended to the much larger IceCube telescope, which now supersedes AMANDA. By exploiting the low photomultiplier noise in the antarctic ice (on average 280 Hz for IceCube), neutrino bursts from nearby supernovae can be identified by the induced collective rise in the pulse rates. Although only a counting experiment, IceCube will provide the world's most precise measurement of the time profile of a neutrino burst near the galactic center. The sensitivity to neutrino properties such as the θ_{13} mixing angle and the neutrino hierarchy are discussed as well as the possibility to detect the deleptonization burst.

Keywords: supernova neutrino IceCube

I. INTRODUCTION

Up to now, the only detected extra-terrestrial sources of neutrinos are the sun and supernova SN1987A. To extend the search to TeV energies and above, neutrino telescopes such as AMANDA and IceCube [1] have been built. It turns out that the noise rates of the light sensors (OMs) in the antarctic ice are very low (~ 700 Hz for AMANDA, ~ 280 Hz for IceCube) opening up the possibility to detect MeV electron anti-neutrinos from close supernovae by an increase in the collective rate of all light sensors. The possibility to monitor the galaxy for supernova with neutrino telescopes such as AMANDA has first been proposed in [2] and a first search has been performed using data from the years 1997 and 1998 [3].

The version of the the supernova data acquisition (SNDAQ) covered in this paper has been introduced for AMANDA in the beginning of the year 2000 and was extended to IceCube in 2007. The AMANDA SNDAQ has been switched off in February 2009. We will investigate data recorded by both telescopes concentrating on the 9 years of AMANDA measurements and make predictions for the expected sensitivity of IceCube.

II. DETECTORS AND DATA ACQUISITION

In AMANDA, the pulses of the 677 OMs are collected in a VME/Linux based data acquisition system which operates independently of the main data acquisition aimed at high energy neutrinos. It counts pulses from every connected optical module in a 20 bit counter in

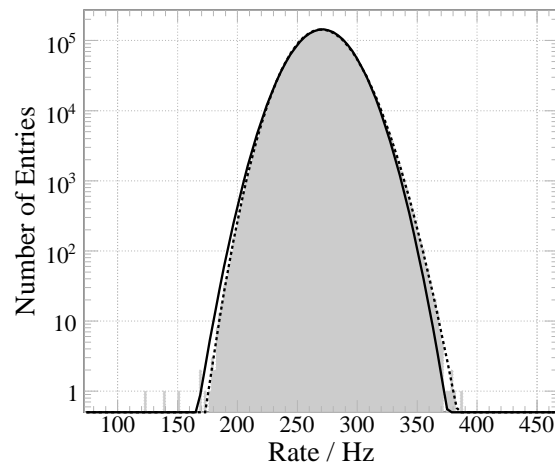


Fig. 1: Rate distribution of a typical IceCube module. The recorded rate distribution (filled area) encompasses about 44 days and has been fitted with a Gaussian (solid line, $\chi^2/N_{\text{dof}} = 56.5$) defined by $\mu = 271$ Hz and $\sigma = 21$ Hz. However, a lognormal function (dotted line, $\chi^2/N_{\text{dof}} = 0.66$) with geometric mean $\mu_{\text{geo}} = 6.4 \ln(\text{Hz})$, geometric standard deviation $\sigma_{\text{geo}} = 0.03 \ln(\text{Hz})$ and a shift of $x_0 = 377$ Hz is much better at describing the data.

fixed 10 ms time intervals that are synchronized by a GPS-clock.

In IceCube, PMT rates are recorded in a 1.6384 ms binning by scalers on each optical module. The information is locally buffered and read out by the IceCube data acquisition system. It then transfers this data to the SNDAQ, which synchronizes and regroups the information in 2 ms bins.

The software used for data acquisition and analysis is essentially the same for AMANDA and IceCube. The data is rebinned in 500 ms intervals and subjected to an online analysis described later. In case of a significant rate increase (“supernova trigger”), an alarm is sent to the Supernova Early Warning System (SNEWS, [4]) via the Iridium satellite network and the data is saved in a fine time binning (10 ms for AMANDA and 2 ms for IceCube).

III. SENSOR RATES

In 500 ms time binning, the pulse distribution of the average AMANDA or IceCube OM conforms only approximately to a Gaussian. It can more accurately be described by a lognormal distribution (see figure 1).

The pulse distributions exhibit Poissonian and correlated afterpulse components contributing with similar strengths. The correlated component is anticorrelated

with temperature and arises from Cherenkov light caused by ^{40}K decays and glass luminescence from radioactive decay chains. A cut at $250\ \mu\text{s}$ on the time difference of consecutive pulses effectively suppresses afterpulse trains, improves the significance of a simulated supernova at 7.5 kpc by approximately 20% and makes the pulse distribution more Poissonian in nature.

IV. EFFECTIVE VOLUMES

Supernovae radiate all neutrino flavors, but due to the relatively large inverse beta decay cross section, the main signal in IceCube is induced by electron anti-neutrinos (see [5]). The rate R per OM can be approximated weighing the energy dependent anti-electron neutrino flux at the earth $\Phi(E_{\bar{\nu}_e})$ (derived from the neutrino luminosity and spectra found in [6]) with the effective area for anti-electron neutrino detection $A_{\text{eff}}(E_{\bar{\nu}_e})$ and integrating over the whole energy range:

$$R = \int_0^\infty dE_{\bar{\nu}_e} \Phi(E_{\bar{\nu}_e}) A_{\text{eff}}(E_{\bar{\nu}_e}), \text{ with}$$

$$A_{\text{eff}}(E_{\bar{\nu}_e}) = n \int_0^\infty dE_{e^+} \frac{d\sigma}{dE_{e^+}}(E_{\bar{\nu}_e}, E_{e^+}) V_{\text{eff},e^+}(E_{e^+}).$$

$\frac{d\sigma}{dE_{e^+}}(E_{\bar{\nu}_e}, E_{e^+})$ is the inverse beta decay cross section, n the density of protons in the ice and $V_{\text{eff},e^+}(E_{e^+})$ the effective volume for positron detection of a single OM.

$V_{\text{eff},e^+}(E_{e^+})$ can be calculated by multiplying the number of Cherenkov photons produced with the effective volume for photon detection $V_{\text{eff},\gamma_{\text{ch}}}$.

By tracking Cherenkov photons in the antarctic ice around the IceCube light sensors [7] and simulating the module response one obtains $V_{\text{eff},\gamma_{\text{ch}}} = 0.104\ \text{m}^3$ for the most common AMANDA sensors and $V_{\text{eff},\gamma} = 0.182\ \text{m}^3$ for the IceCube sensors. With a *GEANT-4* simulation, the amount of photons produced by a positron of an energy E_{e^+} can be estimated to be $N^{\gamma_{\text{ch}}} = 270 E_{e^+}/\text{MeV}$. Consequently, the effective volumes for positrons as a function of their energies are $V_{\text{eff},e^+}^{\text{AMANDA}} = 19.5 E_{e^+} \frac{\text{m}^3}{\text{MeV}}$ and $V_{\text{eff},e^+}^{\text{IceCube}} = 34.2 E_{e^+} \frac{\text{m}^3}{\text{MeV}}$. Uncertainties in the effective volumes derive directly from the uncertainties of the ice models ($\sim 5\%$) and in the OM sensitivities ($\sim 10\%$).

In this paper we assume a supernova neutrino production according to the *Lawrence-Livermore* model [8] as it is the only one that provides spectra for up to 15 s. It gives a mean electron anti-neutrino energy of 15 MeV corresponding to an average positron energy of $(13.4 \pm 0.5)\ \text{MeV}$.

V. ANALYSIS PROCEDURE

A simple investigation of the rate sums would be very susceptible to fluctuations due to variations in the detector response or external influences such as the seasonal variation of muon rates. Medium and long term fluctuations are tracked by estimating the average count rate by a sliding time window. The rate deviation for a collective homogeneous neutrino induced ice illumination is calculated by a likelihood technique. In time bins of 0.5 s and longer, the pulse distributions can be

approximated by Gaussian distributions. For a collective rate increase $\Delta\mu$, the expectation value of the average mean rate μ_i of a light sensor i with relative sensitivity ϵ_i increases to $\mu_i + \epsilon_i \Delta\mu$. The mean value μ_i and its standard deviation σ_i are averaged over a sliding window of 10 min, excluding 15 s before and after the 0.5 s time frame r_i studied. By taking the product of the corresponding Gaussian distributions the following likelihood for a rate deviation $\Delta\mu$ is obtained:

$$\mathcal{L} = \prod_{i=1}^{N_{\text{OM}}} \frac{1}{\sqrt{2\pi} \sigma_i} \exp -\frac{(r_i - (\mu_i + \epsilon_i \Delta\mu))^2}{2\sigma_i^2}.$$

Minimization of $-\ln \mathcal{L}$ leads to:

$$\Delta\mu = \underbrace{\left(\sum_{i=1}^{N_{\text{OM}}} \frac{\epsilon_i^2}{\sigma_i^2} \right)^{-1}}_{= \sigma_{\Delta\mu}^2} \sum_{i=1}^{N_{\text{OM}}} \frac{\epsilon_i (r_i - \mu_i)}{\sigma_i^2}.$$

The data is analyzed in the three time binnings 0.5 s, 4 s and 10 s for the following reasons: First, the finest time binning accessible to the online analysis is 0.5 s. Second, as argued in [9], the neutrino measurements of SN1987A are roughly compatible with an exponential decay of $\tau = 3\ \text{s}$. The optimal time frame for the detection of a signal with such a signature is $\approx 3.8\ \text{s}$. Last, 10 s are the approximate time frame where most of the neutrinos from SN1987A fell.

To ensure data quality, the optical modules are subjected to careful quality checks and cleaning. Those modules with rates outside of a predefined range, a high dispersion w.r.t. the Poissonian expectation or a large skewness are disqualified in real time.

Since SNEWS requests one alarm per 10 days, the supernova trigger is set to $6.3\ \sigma$.

To ensure that the observed rate deviation is homogeneous and isotropic, the following χ^2 discriminant is examined:

$$\chi^2(\Delta\mu) = \sum_{i=1}^{N_{\text{OM}}} \left(\frac{r_i - (\mu_i + \epsilon_i \Delta\mu)}{\sigma_i} \right)^2.$$

We demand the data to conform to a χ^2 -confidence level of 99.9%. However, it was found that the χ^2 cannot clearly distinguish between isotropic rate changes and fluctuations of a significant number of OMs: For e.g. 20% of the OMs record rate increases of about $1\ \sigma$ (≈ 20 pulses/0.5 s), the significance for isotropic illumination can rise above $6\ \sigma$ without being rejected by the χ^2 condition. Still, no method was found that performed better than χ^2 .

VI. EXTERNAL PERTURBATIONS

Figure 2 shows the distribution of the significance $\xi = \frac{\Delta\mu}{\sigma_{\Delta\mu}}$ for AMANDA. From the central limit theorem, one would expect a Gaussian distribution with a width of $\sigma = 1$. This expectation is supported by a background simulation using lognormal representations of individual light sensor pulse distributions. However, one finds that

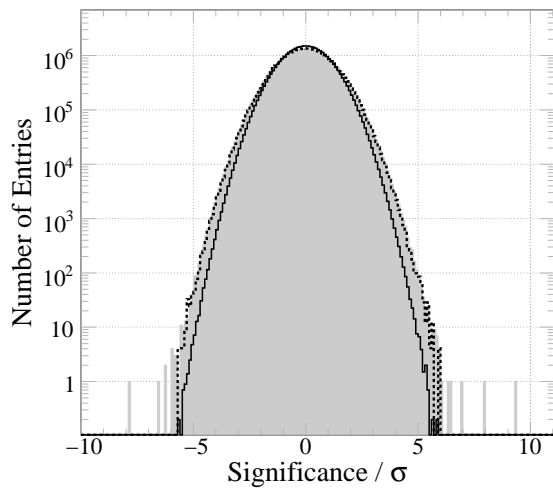


Fig. 2: Significances of AMANDA in 0.5 s time frames. The filled area shows the significance of the data taken in 2002 with a spread of $\sigma = 1.13$. The solid line denotes the initial background simulation ($\sigma \approx 1$) and the dotted line is a toy monte carlo taking into account the fluctuations due to muon rates ($\sigma \approx 1.11$).

the observable is spread wider than expected and exhibits a minor shoulder at high significances.

As this observable is central to the identification of supernovae, its detailed understanding is imperative and a close investigation of these effects is necessary.

Faults in the software were ruled out by simulating data at the most basic level, before entering the SNDAQ. Hardware faults are improbable, as the broadening of the rates is seen both for AMANDA ($\sigma = 1.13$) and IceCube ($\sigma = 1.27$) and the detectors use different and independent power and readout electronics.

One can then check for external sources of rate changes as tracked by magnetometers, rio- and photometers as well as seismometers at Pole. All have been synchronized with the rate measurements of the OMs. Only magnetic field variations show a slight, albeit insignificant, influence on the rate deviation of $-4 \cdot 10^{-5} \frac{\text{Hz}}{\text{nT}}$ for AMANDA. Due to a μ metal wire mesh shielding, the influence on IceCube sensors is smaller by a factor ~ 30 .

It turns out that the main reason for the broadening are fluctuations of the atmospheric muon rates. During 0.5 s, AMANDA detects between $\approx 3.0 \cdot 10^3$ (June) and $\approx 3.4 \cdot 10^3$ (December) sensor hits due to muons. Adding hits from atmospheric muons broadens and distorts the distribution derived from noise rates. A simulation taking into account the muon triggered PMT hits increases the width of the significance distribution to ≈ 1.11 (see figure 2). Although the investigations are still ongoing for IceCube, we expect the larger σ can be ascribed to its lower noise rate leading to a higher resolution and thereby a stronger sensitivity to perturbations.

A Fourier transformation was performed on the data stream. No evidence for periodically recurring events was found, but occasional correlations between subsequent 0.5 s time frames both in the summed noise rate

and the rate deviation could be identified. We determined the mean significance before and after a rate increase exceeding a predefined level. One observes a symmetric correlation in the data mainly between ± 10 s. The origin of the effect, which is present both in AMANDA and IceCube data, is under investigation.

VII. EXPECTED SIGNAL AND VISIBILITY RANGE

A preliminary analysis of AMANDA data from 2000 to 2003 yielded a detection range of $R_{4s} = 14.5$ kpc at the optimal binning of 4 s at an efficiency of 90%, encompassing 81% of the stars of our Galaxy. As signals with exponentially decreasing luminosity (at $\tau = 3$ s) have been used as underlying models, the two other binnings were less efficient with $R_{0.5s} = 10$ kpc (56%) and $R_{10s} = 13$ kpc (75%), respectively.

The rates of the IceCube sensors are stable and uniform across the detector. Scaling the observed rates to the full 80 string detector, a summed rate of $\langle R_{\text{IceCube}} \rangle = (1.3 \cdot 10^6 \pm 1.8 \cdot 10^2)$ Hz is expected. While a single DOM would only see an average rate increase of 13 Hz or 0.65σ , the signal in the whole IceCube detector would be $6.1 \cdot 10^4$ Hz or 34σ for a supernova at 7.5 kpc distance. Using this simple counting method, IceCube would see a supernova in the Magellanic Cloud with 5σ significance.

Figure 3 shows the expected signal in IceCube for a supernova at 7.5 kPc conforming to the *Lawrence-Livermore* model with $\approx 10^6$ registered neutrinos in 15 s and a statistical accuracy of 0.1% in the first 2 s. Assuming $2 \cdot 10^4$ events in Super-Kamiokande (scaled from [10]), one arrives at an accuracy of 1% in the same time frame. While IceCube can neither determine the directions nor the energies of the neutrinos, it will provide worlds best statistical accuracy to follow details of the neutrino light curve. Its performance in this respect will be in the same order as proposed megaton proton decay and supernova search experiments. As the signal is seen on top of background noise, the measurement

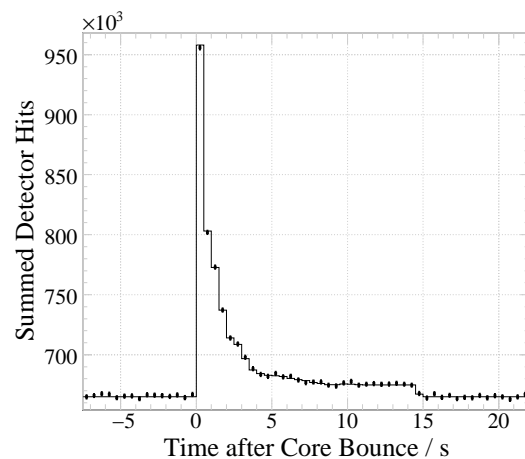


Fig. 3: Expected signal of a supernova at 7.5 kpc in IceCube. The solid line denotes the signal expectation and the bars a randomized simulation.

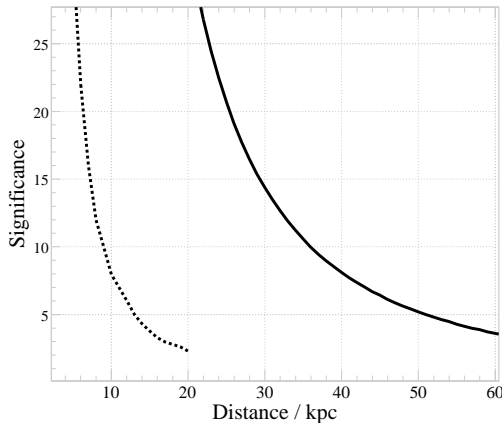


Fig. 4: Supernova detection ranges using 0.5 s time frames. Significances which supernovae conforming to the *Lawrence-Livemore* model would cause as function of their distance. IceCube performance is described by the solid line, AMANDA by the dotted line. Both are given for the 0.5 s binning.

accuracy drops rapidly with distance. Figure 4 shows the significance at which IceCube and AMANDA would be able to detect supernovae.

VIII. DELEPTONIZATION PEAK AND NEUTRINO OSCILLATIONS

As mentioned before, the signal seen by AMANDA and IceCube is mostly dominated by electron anti-neutrinos with a small contribution by electron neutrino scattering, thereby leading to a sensitivity which is strongly dependent on the neutrino flavor and is thus sensitive to neutrino oscillations.

As the neutrinos pass varying levels of density within the supernova, the flux of electron and electron anti-neutrinos Φ released is different from the initial flux Φ^0 produced during the collapse:

$$\begin{aligned}\Phi_{\nu_e} &= p \Phi_{\nu_e}^0 + (1-p) \Phi_{\nu_x}^0, \\ \Phi_{\bar{\nu}_e} &= \bar{p} \Phi_{\bar{\nu}_e}^0 + (1-\bar{p}) \Phi_{\bar{\nu}_x}^0.\end{aligned}$$

The survival probability p/\bar{p} for the $\nu_e/\bar{\nu}_e$'s varies with the mass hierarchy and the mixing angle θ_{13} [11]:

neutrino oscillation parameters	p	\bar{p}
$m_2^2 < m_3^2, \sin^2 \theta_{13} > 10^{-3}$	$\approx 0\%$	69%
$m_1^2 > m_3^2 < 0, \sin^2 \theta_{13} > 10^{-3}$	31%	$\approx 0\%$
any hierarchy, $\sin^2 \theta_{13} < 10^{-5}$	31%	69%

At the onset of the supernova neutrino burst during the prompt shock, a ~ 10 ms long burst of electron neutrinos gets emitted when the neutron star forms. As the shape and rate of this burst is roughly independent of the properties of the progenitor stars, it is considered as a standard candle, allowing one to determine neutrino properties without knowing details of the core collapse.

The first 0.7 s of a supernova signal were modeled after [12]. Figure 5 shows the expectation for a supernova

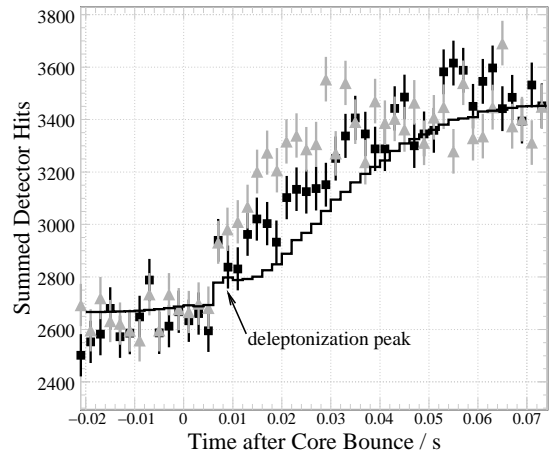


Fig. 5: Neutrino signals of a supernova at 7.5 kpc distance modified by oscillations as seen in IceCube.

The line shows the expectation without neutrino oscillations, the squares show the simulated signal for the normal mass hierarchy with $\sin^2 \theta_{13} > 10^{-3}$ ($\sin^2 \theta_{13} < 10^{-5}$ lies nearly on the same line) and the triangles show the signal for inverted mass hierarchy at $\sin^2 \theta_{13} > 10^{-3}$.

at a distance of 7.5 kpc in the 2 ms binning of IceCube. Due to statistics and the rising background from the starting electron anti-neutrino signal, the identification of the neutronization burst is unlikely at this distance. However, with a supernova at 7.5 kpc one might be able to draw conclusions for the mass hierarchy, depending on the reliability of the models.

IX. CONCLUSIONS AND OUTLOOK

With 59 strings and 3540 OMs installed, IceCube has reached 86% of its final sensitivity for supernova detection. It now supersedes AMANDA in the SNEWS network. With the low energy extension DeepCore, IceCube gains 360 additional OMs with a $\sim 30\%$ higher quantum efficiency (rates ~ 380 Hz). These modules have not been considered in this paper.

REFERENCES

- [1] A. Karle *et al.* arXiv:0812.3981
- [2] F. Halzen, J. E. Jacobsen and E. Zas *Phys. Rev.*, D49:1758–1761, 1994 hep-ph/9307240
- [3] J. Ahrens *et al.* *Astropart. Phys.* 16:345–359, 2002, astro-ph/0105460
- [4] P. Antonioli *et al.* *New J. Phys.* 6:114, 2004, astro-ph/0406214
- [5] W. C. Haxton. *Phys. Rev.*, D36:2283, 1987
- [6] M. Th. Keil, G. G. Raffelt and H.-T. Janka. *Astrophys. J.*, 590:971–991, 2003, astro-ph/0208035
- [7] M. Ackermann *et al.* *J. Geophys. Res.*, 111:D13203, 2006, astro-ph/0702108
- [8] T. Totani, K. Sato, H. E. Dalhed and J. R. Wilson *Astrophys. J.*, 496:216–225, 1998 astro-ph/9710203
- [9] J. F. Beacom and P. Vogel *Phys. Rev.* D60:033007, 1999, astro-ph/9811350
- [10] M. Ikeda *et al.* *Astrophys. J.*, 669:519–524, 2007, arXiv:0706.2283
- [11] A. Dighe. *Nucl. Phys. Proc. Suppl.*, 143:449–456, 2005, hep-ph/0409268
- [12] F. S. Kitaura, Hans-Thomas Janka and W. Hillebrandt *Astron. Astrophys.* 450:345–350, 2006, astro-ph/0512065